Wavelet Transforms and Atmospheric Turbulence

Lonnie Hudgins,[1] Carl A. Friehe,[2] and Meinhard E. Mayer[3]
[1]*Northrop Corporation, Hawthorne, California 90251-5032*
[2]*Department of Mechanical Engineering, University of California, Irvine, California 92717*
[3]*Department of Physics, University of California, Irvine, California 92717*
(Received 5 May 1993)

Wavelet cross spectra and cross scalograms are used to analyze the time-scale structure of bivariate turbulence data from the boundary layer over the ocean. The cross scalogram for the streamwise and vertical turbulent velocity components shows a highly intermittent pattern with significant contributions of opposite signs appearing at two specific scales, ~ 60 m and ~ 2 km, believed to be related to small-scale turbulent mixing and large-scale secondary flow in the boundary layer.

PACS numbers: 47.27.Jv, 02.30.Nw, 02.70.Hm, 92.10.Lq

The purpose of this Letter is to bring to the attention of the physics community a recent technique of time-scale bivariate analysis, based on *wavelet transforms*, which we apply to the study of atmospheric turbulence.

Fourier and correlation analysis techniques have traditionally provided spatial and temporal decompositions of individual turbulence variables into scales averaged over the data record. With the increasing popularity of wavelet methods for the analysis of phenomena which exhibit scaling behavior, including turbulence (see, e.g., [1–5]), we compared the two methods.

We are specifically interested in the wavelet analysis products of certain variables, because in the Reynolds-averaged sense of turbulence the important transfer terms (momentum, heat, and species) appear as averaged products of the instantaneous velocity components, temperature, and concentrations. These were usually treated by Fourier cross-spectral and cross-correlation techniques. We develop an equivalent *wavelet cross-spectrum* technique, and compare it to the Fourier case.

Since the wavelet transform yields scale estimations which are better than those of Fourier methods, we were motivated to study the intermittency of the turbulent fluxes by examining the time-scale representation of the wavelet cross spectrum, which we call the *wavelet cross scalogram*. In atmospheric flows one cannot repeat the experiment in the spirit of forming ensemble averages of Fourier periodograms to obtain smoothed spectral amplitudes. We were therefore interested in the relative merit of wavelets for smoothing for a finite data segment.

These new techniques were applied to high Reynolds-number data from the turbulent boundary layer over the ocean. Both univariate data and bivariate data of velocity components and temperature were analyzed. The bivariate analysis was performed on the vertical and longitudinal wind components (momentum transfer), and the vertical component with temperature (heat flux).

Further details of the work summarized here are contained in the first author's thesis [6], where one can find a more complete bibliography. A preliminary report was presented at the Toulouse Wavelet Conference in 1992 [7].

Wavelet and Fourier spectra: basic definitions.—A function $\Psi \in L^1 \cap L^2(\mathbb{R})$, whose Fourier transform $\widehat{\Psi}$ satisfies $c_\Psi = \int |\widehat{\Psi}(\omega)|^2 |\omega|^{-1} d\omega < \infty$, is called an *(admissible) wavelet*, The constant c_Ψ, which obviously depends on the wavelet Ψ, is called the *admissibility constant.*

A wavelet Ψ can be thought of as a bandpass filter because its Fourier transform is mainly concentrated on some frequency interval. A family of filters is defined in terms of Ψ by the operation of dilation or scaling. For any $s \in \mathbb{R}$, let $\Psi_s(t) = \sqrt{|s|}\, \Psi(st)$. The factor $\sqrt{|s|}$ keeps the L^2 norm of each filter independent of s. In most of the existing literature on wavelets, the *scale length* parameter a appears in the denominator, so that $\Psi_a(t) = 1/\sqrt{|a|}\Psi\,(t/a)$, for $a \neq 0$. In the Fourier context, a is the analog of wavelength. We use the variable $s = 1/a$, which is analogous to the wave number and call it *scale number.* We will allow s to take negative values, whereas a is often assumed to be strictly positive. Since the Fourier transform of Ψ_s is equal to $\widehat{\Psi}_s(\omega) = 1/\sqrt{|s|}\widehat{\Psi}\,(\omega/s)$, the parameter s linearly scales both the center frequency and the width of the pass band.

If Ψ is an admissible wavelet, and f is square integrable, then the *wavelet transform* $\mathcal{W}_f(s,\tau)$ of f at time τ and scale number s is defined by

$$\mathcal{W}_f(s,\tau) = \int f(t)\Psi_s(t-\tau)\, dt. \tag{1}$$

At each fixed scale s we get a version of $f(t)$, bandpassed by the filter Ψ_s. To see this in the frequency domain, we Fourier transform in τ: $\widehat{\mathcal{W}_f}(s,\omega) = \hat{f}(\omega)\widehat{\Psi}_s(-\omega)$.

The wavelet transform is norm preserving, but the range space is $L^2(\mathbb{R}^2)$ since $\mathcal{W}_f$ is a function of two real variables. Formally, we have *Parseval's relation for wavelets:* If f belongs to $L^2(\mathbb{R})$,

$$\|f\|^2 = \frac{1}{c_\Psi}\int ds \int d\tau\, |\mathcal{W}_f(s,\tau)|^2. \tag{2}$$

In polarized form, if f and g belong to $L^2(\mathbb{R})$, then

$$\langle f, g\rangle = \frac{1}{c_\Psi}\int ds \int d\tau\, \mathcal{W}_f^*(s,\tau)\mathcal{W}_g(s,\tau). \tag{3}$$

The inverse wavelet transform is (for almost all t)

0031-9007/93/71(20)/3279(4)$06.00

$$f(t) = \frac{1}{c_\Psi} \int\int ds\, d\tau\, \mathcal{W}_f(s,\tau)\Psi_s{}^*(\tau - t). \quad (4)$$

For Fourier transforms, the "power spectrum" is $\mathcal{P}_f(\omega) = |\hat{f}(\omega)|^2$, and the "cross spectrum" of the pair f, g is $\mathcal{C}_{fg}(\omega) = \hat{f}(\omega)^* \hat{g}(\omega)$. We introduce the analogous *wavelet power spectrum and cross spectrum.* The following definitions were inspired by work of Mahrt and collaborators [8–10], and are close to those of Meneveau (Ref. [4]).

If $\mathcal{W}_f(s,\tau)$ is the wavelet transform of f with a wavelet Ψ, then the *wavelet power spectrum* of f is defined as

$$\mathcal{P}_f^w(s) = \int d\tau\, |\mathcal{W}_f(s,\tau)|^2. \quad (5)$$

In polarized form, for a pair of square-integrable functions f and g, the *wavelet cross spectrum* is

$$\mathcal{C}_{fg}^w(s) = \int d\tau\, \mathcal{W}_f^*(s,\tau)\mathcal{W}_g(s,\tau). \quad (6)$$

The integrand in the right-hand side is the time-scale decomposition of the wavelet cross spectrum, and its density plot in the τ, s plane is what we called the *cross scalogram.* While scalograms have been used to represent individual variables, the use of cross scalograms for bivariate analysis is the primary contribution of this work.

When f, g, and Ψ are real, the wavelet cross spectrum is real, and we make no distinction between the wavelet cross spectrum and the wavelet co-spectrum.

The function $\mathcal{W}_f$ on $\mathbb{R}^2$ contains much redundant information. If the basic wavelet Ψ satisfies certain conditions [11], the domain of $\mathcal{W}_f$ may be restricted to a countable subset, and the resulting wavelet family is an orthonormal basis for L^2. When this happens, all of the formulas above remain valid, but the integrals can often be replaced by summations. The most common such restriction involves $s \in \{2^{-n}\}$ for integer n, and produces discrete spectra at one-octave intervals.

Finally, to relate the wavelet power spectrum of f to the Fourier power spectrum $\mathcal{P}_f$, we note that

$$\mathcal{P}_f^w(s) = \frac{1}{2\pi} \int d\omega\, \mathcal{P}_{\Psi_s}(\omega)\mathcal{P}_f(\omega), \quad (7)$$

i.e., it is the Fourier power spectrum averaged by the power spectrum of the bandpass filter. Similarly, the wavelet cross spectrum of f and g is the Fourier cross spectrum averaged by $\mathcal{P}_{\Psi_s}$:

$$\mathcal{C}_{fg}^w(s) = \frac{1}{2\pi} \int d\omega\, \mathcal{P}_{\Psi_s}(\omega)\mathcal{C}_{fg}(\omega). \quad (8)$$

The scale dependence is contained in the power spectrum of the wavelet, $\mathcal{P}_{\Psi_s}(\omega)$.

Data collection.—The data used in the analysis were obtained in the horizontally homogeneous boundary layer of the lower atmosphere over the open ocean. The Reynolds number is estimated to be at least 10^6 and an extensive Kolmogorov inertial subrange is expected.

Measurements of the three components of the wind velocity and the instantaneous air temperature were made at about 200 km west of San Diego, from R/P FLIP. The instrument package, situated 8 m above the ocean, consisted of a three-path sonic anemometer and a 130 μm thermistor bead. The bandwidth of the anemometer was dc to 10 Hz, while that of the thermistor was dc to 5 Hz. The data were recorded with a 16-bit resolution at 32 Hz with 16 Hz anti-aliasing filters. Conversion from frequency to scale was made using Taylor's hypothesis with the mean wind speed of 12 m/s.

Results.—The data were analyzed using both fast Fourier (FFT) and wavelet transforms, making use of a cubic spline wavelet (see [12]), Fig. 1, chosen because it represents a good compromise between time localization, frequency localization, and peak-to-sidelobe ratio, while maintaining phase linearity [6].

Spectra and co-spectra were computed with a 128-point FFT, using maximally overlapped ensemble averaging. The means of the signals were removed. This produced 64 equally spaced spectral estimates between 0 and 16 Hz. For comparison, 64 wavelet spectral estimates were also calculated, spaced logarithmically with 8 estimates per octave, from 1/16 Hz to 16 Hz. To extend this

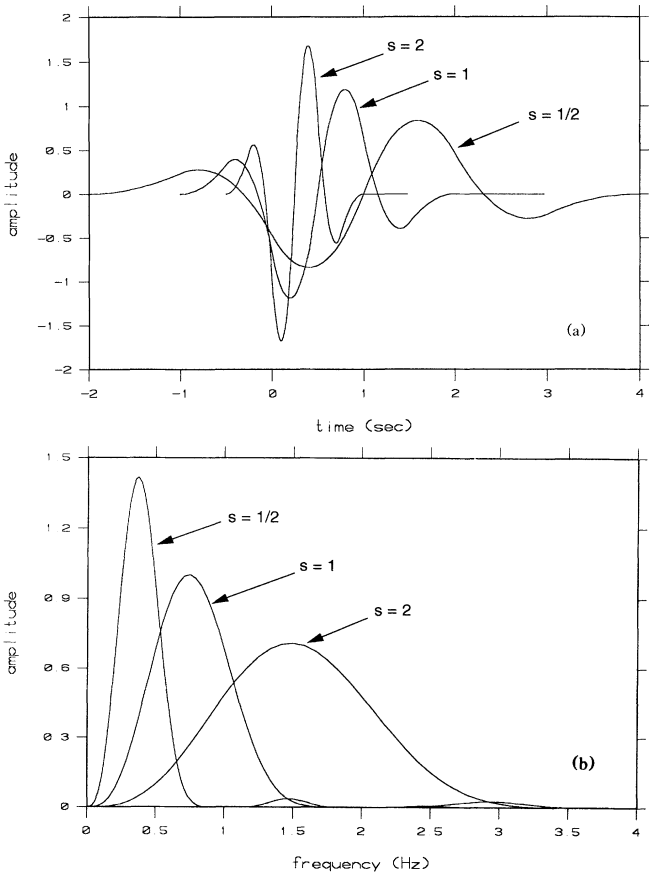

FIG. 1. Cubic spline wavelet in both the time (a) and frequency (b) domains at three dilations: $s = 1, 1/2, 2$.

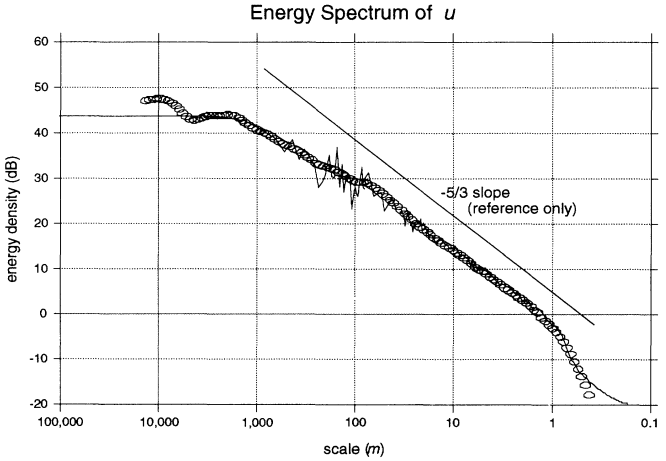

FIG. 2. Fourier (solid line) and wavelet (circles) energy spectra of the streamwise horizontal velocity component u. Also shown is the $-5/3$ slope corresponding to the Kolmogorov inertial subrange.

comparison over a wider range, the original data record was re-sampled at 128 Hz, 8 Hz, 2 Hz, 1/2 Hz, and 1/8 Hz. For each new sample rate, 64 spectral estimates were computed with both FFT and wavelet transforms. The resulting spectra were pieced together on a logarithmic scale covering approximately four decades.

The Fourier power spectrum of the streamwise horizontal velocity component u and its wavelet equivalent are shown in Fig. 2. The wavelet method seems to give a better smoothed representation of the spectrum. More detail is shown at low frequencies while retaining the overall shape at higher frequencies. The power-law slope of $-5/3$ of the Kolmogorov inertial subrange is also shown, and agrees with the data for frequencies from ~ 0.1 to 10 Hz, the limit of the anemometer.

The time-bandwidth product of the cubic-spline wavelets is greater than that of the windowed sine functions of the Fourier basis. This accounts for the increased smoothness of the wavelet spectra. Generally, this property would tend to obscure features which are sharply localized in the frequency domain. However, the structures we have found here do not appear to be adversely affected by the smoothing. At the same time, the logarithmic frequency spacing of the wavelet transform provides arbitrarily high resolution at low frequencies. To obtain an equivalent resolution with a Fourier analysis, one must either use very long FFT's, or decimate the data by some large factor as we have done here. Either of these lead to increased compute time for the FFT, whereas for certain classes of wavelet transforms the "decimation" is automatic, and comes for free.

We show two representative co-spectra in Fig. 3: that of $u \times w$ (momentum flux) and $w \times T$ (heat flux), where u, w are the streamwise and vertical components of the velocity, respectively, and T is the temperature. In order to show the variation in co-spectral "energy" as a

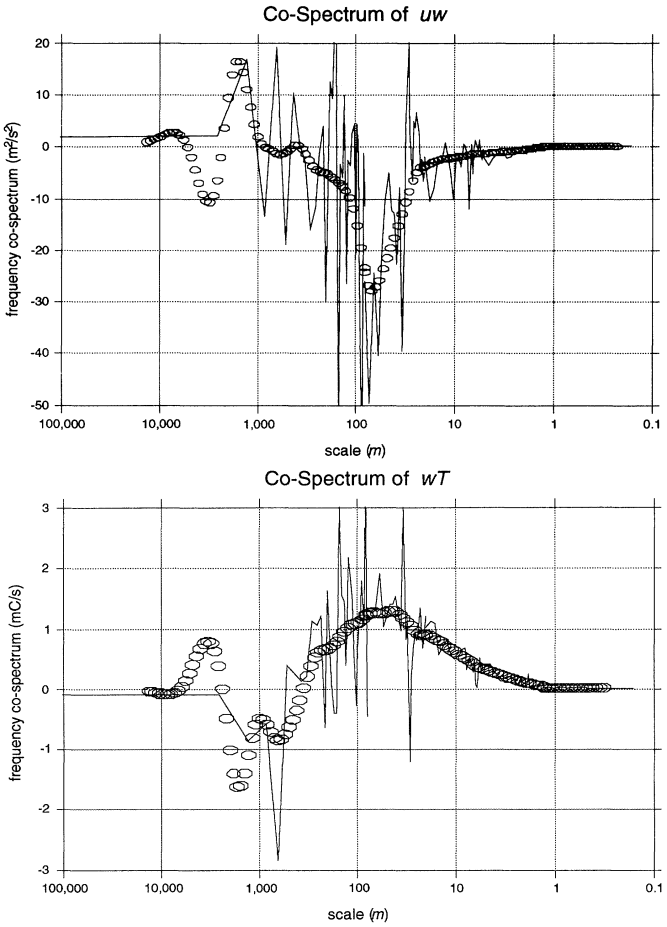

FIG. 3. The $u \times w$ and $w \times t$ co-spectra. The solid line shows the co-spectral estimate via Fourier analysis; the circles represent the wavelet co-spectra. (Note: The co-spectra are presented in area-preserving form on semilogarithmic scales.)

function of frequency, we use the method of plotting the co-spectra in area-preserving form on semilogarithmic scales. Here the wavelet co-spectra resolve the bimodal feature of the momentum and heat fluxes. The momentum flux has negative values in a region centered at about 60 m, while there is a positive region around 2 km. The opposite is true for the heat flux. The Fourier co-spectra show a slight indication of the longer wavelength mode.

Plotting the first moment of the wavelet cross transform is also an effective way to show the intermittency in the two-dimensional contour plots—the cross scalograms. To illustrate this, such a cross scalogram is shown in Fig. 4. [6] The instantaneous product of the u and w fluctuations is depicted as a time series at the top of the graph. Below it is the wavelet cross transform $\mathcal{W}_u(s,\tau)\overline{\mathcal{W}_w(s,\tau)}$. The vertical axis in the lower plot is the scale number, so the small length scales appear at the top. Positive regions are in shades of red, passing from white, to pink, through deep red to black; nega-

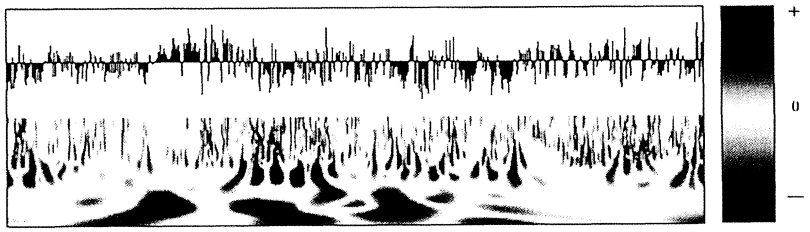

FIG. 4. Wavelet cross scalogram showing approximately 250 s of data. The upper half shows the time series of the instantaneous product $u \times w$; the lower half is a color plot of its wavelet cross spectrum, as explained in the text. The relative spectral levels are indicated by the color scale on the right. The time in the abscissa is common for both plots.

tive regions use shades of blue. The positive and negative extrema are both colored black, but are surrounded by regions of red or blue, respectively. The dark blue oval-shaped features to the left of center are the 60 m structures, while the larger red and blue shapes below them represent 2 km structures. The color plot displays clearly the sign change in the spectra, corresponding to Fig. 3. Notice the highly intermittent features, a characteristic which is very difficult (if not impracticable) to analyze with Fourier transforms. To resolve either of these structures with Fourier techniques, one would have to know their size *a priori,* and set the length of the window function accordingly. But since the 60 m and 2 km structures are so different in size, this cannot be accomplished simultaneously for both. In contrast, the wavelet transform uses a dynamically adjustable "window," and is thus capable of resolving all scales simultaneously.

To explain the bimodal structure qualitatively, we note that since the sea was slightly warmer than the air, one can expect a net upward (positive) heat flux from the sea to the air; similarly, the sea surface is a sink of horizontal momentum of the wind, and one expects a downward (negative) momentum ($u \times w$) flux. These qualitative features are supported by the present results; the integrals (areas) of the co-spectra are positive for $w \times T$ and negative for $u \times w$. The co-spectral analysis breaks down the integral (average) fluxes into various frequencies or scales. From Fig. 3 we see that the main contributions to the co-spectral "energies" are at scales that peak around 60 m. This scale corresponds to the surface-layer turbulence scale, where most of the (positive) heat transfer and (negative) momentum transfer are taking place. However, at large scales of about 2 km, transfers of opposite sign occur and represent upward momentum flux, counter to the mean wind gradient. It is believed that these are associated with the large-scale features of the boundary layer, such as horizontal roll vortices. Overall (i.e., integrated co-spectra), counter-gradient transfer in turbulence is not new, but with the wavelet analysis we have been able to detect both gradient and counter-gradient transfer as a function of scale in the flow.

In conclusion, the analysis of turbulent fluxes shows that wavelet cross-scalogram analysis can be extremely useful in representing the time-scale structure of bivariate data. When integrated over time, the wavelet method provides a better view of the frequency-amplitude spectra and co-spectra. In particular, low frequency variations are well resolved, and in this case, a bimodal structure of the averaged turbulent fluxes was revealed.

The intermittent localized features of the flux fields are clearly shown in the wavelet cross-scalogram plots. The method holds promise for examining the structure of turbulence, and perhaps other random fields where bivariate phenomena are also important.

L.H. would like to acknowledge a Northrop Corporation fellowship, which enabled him to complete his Doctorate at U.C. Irvine. C.A.F. would like to thank Dr. R. Weller of the Woods Hole Oceanographic Institution for the opportunity to participate in the R/P FLIP cruise, and to acknowledge the support of ONR Grant No. N00014-J-0190, NSF Grants No. ATM-8715619, No. 9024436, and the U.C. INCOR program.

[1] R. Everson, L. Sirovich, and K. R. Sreenivasan, Phys. Lett. A **145**, 314 (1990).
[2] M. Farge and G. Rabreau, C.R. Acad. Sci. Paris, Ser. II **307**, 1479 (1988).
[3] M. Farge, Annu. Rev. Fluid Mech. **24**, 395–457 (1992).
[4] C. Meneveau, J. Fluid Mech. **232**, 469 (1991).
[5] M. Yamada and K. Ohkitani, Fluid Dyn. Res. **8**, 101–105 (1991).
[6] L. Hudgins, thesis, University of California, Irvine, March 1992.
[7] L. Hudgins, C. Friehe, and M. E. Mayer, in *Proceedings of the International Conference on Wavelets, Toulouse, 1992,* edited by Y. Meyer and S. Roques (Edition Frontières, Gif-sur-Yvette, 1993), pp. 491–498.
[8] L. Mahrt, J. Atmos. Sci. **48**, 472 (1991).
[9] N. Gamage and L. Mahrt, Department of Atmospheric Sciences, OSU, Technical Report, February 1991 (unpublished).
[10] L. Mahrt and J. Howell, in Proceedings of the Conference on Turbulent Shear Flows, Technical University, Munich, 9–11 September 1991 (unpublished).
[11] I. Daubechies, *Ten Lectures on Wavelets* (AMS, Providence, 1992).
[12] C. Chui, *An Introduction to Wavelets* (Academic Press, New York, 1992).

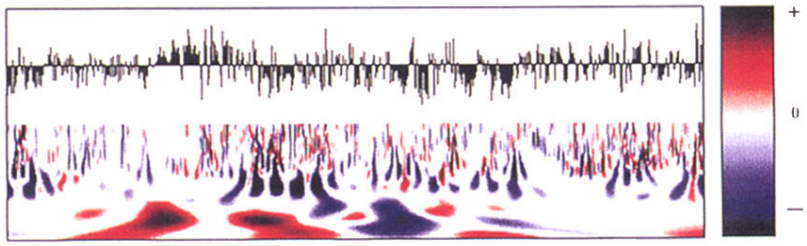

FIG. 4. Wavelet cross scalogram showing approximately 250 s of data. The upper half shows the time series of the instantaneous product $u \times w$; the lower half is a color plot of its wavelet cross spectrum, as explained in the text. The relative spectral levels are indicated by the color scale on the right. The time in the abscissa is common for both plots.